Journal of Molecular Structure 1198 (2019) 126782

Contents lists available at ScienceDirect

Journal of Molecular Structure

journal homepage: http://www.elsevier.com/locate/molstruc

Synthesis and structural features of N-[(2-(trimethylsilyl)oxy)phenyl]-arylsulfonamides

Alexey Yu Nikonov, Irina V. Sterkhova*, Valeriy Yu Serykh, Nikita A. Kolyvanov, Natalya F. Lazareva

A. E. Favorskii Irkutsk Institute of Chemistry, Siberian Division of Russian Academy of Sciences, 1 Favorskii Street 664033, Irkutsk, Russia

ARTICLE INFO

Article history:
Received 26 February 2019
Received in revised form
21 June 2019
Accepted 4 July 2019
Available online 31 July 2019

Keywords:
N-[(2-(trimethylsilyl)oxi)phenyl]
sulfonamides
Crystal structure
FTIR spectroscopy
H-bonding
DFT calculations

ABSTRACT

N-[(2-(Trimethylsilyl)oxy)phenyl]-4-methylbenzenesulfonamide and N-[(2-trimethylsilyloxy)phenyl]-4-chlorobenzenesulfonamide were prepared by two different methods. Their structures were studied by X-ray single-crystal analysis and DFT calculations including MO and NBO analyses. Self-association in solutions was shown by FTIR-spectroscopy.

1. Introduction

Sulfonamides $RSO_2NR'R''$ (R, R′, R″ = Alk, Ar, Hetaryl) attract much attention due to the important role they play in organic and medicinal chemistry. Thus, sulfonamides are efficient directing groups in various metal-catalyzed reactions [[1, 2] and refs. therein] and are used as protecting groups for amines [[3–5] and refs. therein].

Sulfonamides display a wide spectrum of biological activity, such as antibacterial, antiviral, anticancer, antifungal, antiinflammatory, antituberculosis, carbonic anhydrase inhibition, antimalarial, antiparasitic, anticonvulsant, antidepressant activities [6–16], and are used as precursors in drug production [17–19]. To a large extent, the biological activity of sulfonamides is due to their possibility to form non-covalent bonds, like hydrogen and halogen bonds, complexation with metal centers of proteases, π-bonding with aromatic donors, etc. [20–26]. Silicon is isosteric to carbon [27], and incorporation of silicon bioisosteres into the known drug molecules can modify their biological activity by increasing the therapeutic effect and reduce the toxicity [28,29].

During our research on the chemistry of fluorinated and silylated amides and sulfonamides, we obtained a lot of their derivatives, whose conformational and supramolecular structure was studied by X-ray analysis, IR spectroscopy and quantum chemical calculations [30–33]. Such an integrated approach, which includes both experimental and theoretical studies, is often used to study organic compounds including silicon-containing derivatives [34–37]. Recently, we synthesized a series of silylated amides $Me_3SiNHCO(SO_2)R$ (R = Me, CF_3, Ph) [38,39] and analyzed their structural features.

The purpose of this work was to investigate the structural features of two polyfunctional Si-containing arylsulfonamides 2-$Me_3SiOC_6H_4NHSO_2C_6H_4$-X [X = CH_3 (**1**), Cl (**2**)]. Compound **1** was obtained by the reaction of N-(2-hydroxyphenyl)-4-methylbenzenesulfonamide **3** with Me_3SiCl or hexamethyldisilazane (Scheme 1). It should be noted that silylation of **3** with excess of hexamethyldisilazane lead to formation of a 1:1 mixture of compound **1** and N-(trimethylsilyl)-N-[(2-(trimethylsilyl)oxy) phenyl]-4-methylbenzenesulfonamide **4**.

2. Experimental

All experiments with O-silyl derivatives were carried out under dry argon atmosphere using standard Schlenk techniques. Solvents

* Corresponding author.
E-mail address: irina_sterkhova@irioch.irk.ru (I.V. Sterkhova).

https://doi.org/10.1016/j.molstruc.2019.07.029
0022-2860/

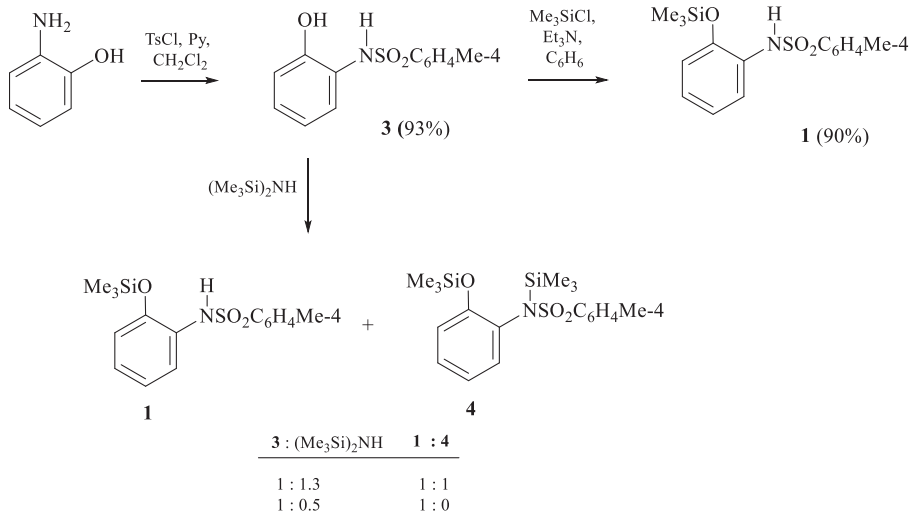

Scheme 1. Compound **2** was synthesized by the reaction of 2-(trimethylsilyloxy)aniline **5** and 4-chlorobenzenesulfonyl chloride in benzene at 40–50 °C (Scheme 2).

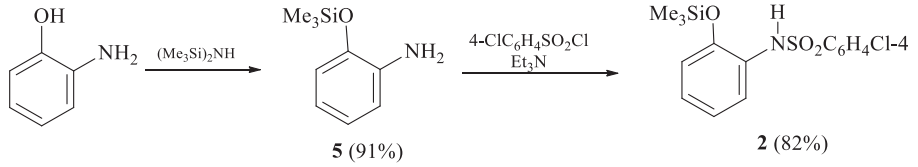

Scheme 2. The structure of compounds **1** and **2** was investigated by NMR and IR spectroscopy, and X-ray diffraction analysis.

were dried and freshly distilled under argon prior to use [40].

2.1. Synthesis and crystallization

2.1.1. N-(2-hydroxyphenyl)-4-methylbenzenesulfonamide *3*

Compound **3** was synthesized as described in Refs. [41,42]. To the vigorously stirred emulsion of *o*-aminophenol (3 g, 27.5 mmol) and pyridine (2.2 g, 27.8 mmol) in CH_2Cl_2 (50 ml) the solution of tosyl chloride (5.3 g, 27.8 mmol) in CH_2Cl_2 (30 ml) was added dropwise. After stirring for 2 h at room temperature, the mixture was washed with water (100 ml), the organic layer was separated, dried over magnesium sulfate, filtered and concentrated in vacuum to give crude solid residue. After crystallization from CH_2Cl_2, pure N-(2-hydroxyphenyl)-4-methylbenzenesulfonamide **3** was obtained in ~93% yeld (6.7 g). ^{1}H NMR ($CDCl_3$, δ, ppm): 2.38 (s, 3H, $C\underline{H}_3C_6H_4SO_2$), 6.42 (br. s, 1H, OH), 6.56 (s, 1H, NH), 6.72 (m, 1H, $C_6\underline{H}_4OH$), 6.81 (m, 1H, $C_6\underline{H}_4OH$), 6.90 (m, 1H, $C_6\underline{H}_4OH$), 7.06 (m, 1H, $C_6\underline{H}_4OH$), 7.23 (m, 2H, 4-$CH_3C_6\underline{H}_4$), 7.54 (m, 1H, 4-$CH_3C_6\underline{H}_4$), 7.60 (m, 2H, 4-$CH_3C_6\underline{H}_4$). Anal. calcd. for $C_{13}H_{13}NO_3S$: C, 59.30; H, 4.98; N, 5.32. Found: C, 58.92; H, 4.67; N, 5.41.

2.1.2. N-[(2-(Trimethylsilyl)oxy)phenyl]-4-methylbenzenesulfonamide (*1*) and N-(trimethylsilyl)-N-[(2-(trimethylsilyl)oxy)phenyl]-4-methylbenzenesulfonamide (*4*)

a) Chlorotrimethylsilane (0.9 g, 8.2 mmol) in 10 ml of benzene was added dropwise under stirring to a solution of N-(2-hydroxyphenyl)-4-methylbenzenesulfonamide **3** (2.1 g, 8 mmol) in 30 ml of benzene with 1 g of triethylamine. The reaction mixture was stirred for 6 h with moderate heating (40–50 °C). After cooling to room temperature a precipitate of $Et_3N{\cdot}HCl$ was filtered off and washed with 50 ml of benzene. The solvent was evaporated in vacuo. A residue was washed with hexane (10 ml) and dried in vacuo. Resulted product was melted and after cooling the crystals of (**1**) were obtained in 90% yield.

b) The mixture of N-(2-hydroxyphenyl)-4-methylbenzenesulfonamide **3** (2.5 g, 9.5 mmol) and the excess of hexamethyldisilazane (2.0 g, 12.4 mmol) was refluxed for 24 h. Resulted product was dried in vacuo to give 3.4 g of viscous residue. NMR analysis revealed the product as a mixture of N-[(2-(trimethylsilyl)oxy)phenyl]-4-methylbenzenesulfonamide (**1**) and N-(trimethylsilyl)-N-[(2-(trimethylsilyl)oxy)phenyl]-4-methylbenzenesulfonamide (**4**) with ratio 1:1 with total conversion of **3** about 97%. Reaction of 2.1 g of **3** (8 mmol) with 0.65 g (4 mmol) of hexamethyldisilazane resulted in obtaining of almost pure compound **1** in ~97% yield (2.62 g).

N-[(2-(Trimethylsilyl)oxy)phenyl]-4-methylbenzenesulfonamide (**1**). ^{1}H NMR ($CDCl_3$, δ, ppm): 0.16 (s, 9H, $(C\underline{H}_3)_3Si{-}O$), 2.35 (s, 3H, $C\underline{H}_3C_6H_4SO_2$), 6.66 (m, 1H, ArO), 6.86–6.96 (m, 2H, ArO), 7.18 (m, 2H, 4-$CH_3C_6\underline{H}_4$), 7.54 (m, 1H, ArO), 7.61 (m, 2H, 4- $CH_3C_6\underline{H}_4$). ^{13}C NMR ($CDCl_3$, δ, ppm): 0.75 ($(\underline{C}H_3)_3Si{-}O$), 21.35 ($\underline{C}H_3C_6H_4SO_2$), 117.42 ($C_3$), 121.75 ($C_6$), 121.95 ($C_5$), 125.33 ($C_4$), 127.34 ($C_m$ 4-$CH_3C_6H_4$), 127.93 (C_1), 129.63 (C_o 4-$CH_3C_6H_4$), 136.68 (C_p 4-$CH_3C_6H_4$), 143.85 (C_i 4-$CH_3C_6H_4$), 145.88 (C_2). ^{29}Si NMR ($CDCl_3$, δ, ppm): 21.8 ($(CH_3)_3Si{-}O$). Anal. calcd. for $C_{16}H_{21}NO_3SSi$: C, 57.28; H, 6.31; N,4.17. Found: C, 57.61; H, 6.54; N, 4.11.

N-(Trimethylsilyl)-N-[(2-(trimethylsilyl)oxy)phenyl]-4-methylbenzenesulfonamide (**4**).

^{1}H NMR ($CDCl_3$, δ, ppm): 0.11 (s, 9H, $(CH_3)_3Si{-}O$), 0.27 (s, 9H, $(CH_3)_3Si{-}N$) 2.36 (s, 3H, $C\underline{H}_3C_6H_4SO_2$), 6.62 (m, 1H, ArO), 6.82–6.88 (m, 2H, ArO), 7.13 (m, 2H, 4-$CH_3C_6H_4$), 7.54 (m, 1H, ArO), 7.61 (m, 2H, 4-$CH_3C_6H_4$). ^{13}C NMR ($CDCl_3$, δ, ppm): 0.13 ($(\underline{C}H_3)_3Si{-}O$), 1.03 ($(\underline{C}H_3)_3Si{-}N$) 21.40 ($\underline{C}H_3C_6H_4SO_2$), 117.72 ($C_3$), 121.75 ($C_6$), 121.95

(C_5), 120.86 (C_4), 127.34 (C_m 4-$CH_3C_6H_4$), 128.17 (C_1), 133.54 (C_o 4-$CH_3C_6H_4$), 136.48 (C_p 4-$CH_3C_6H_4$), 142.50 (C_i 4-$CH_3C_6H_4$), 153.21 (C_2). ^{29}Si NMR ($CDCl_3$, δ, ppm): 18.4 ($(CH_3)_3Si{-}O$), 13.5 ($(CH_3)_3Si{-}N$).

2.1.3. N-[(2-(Trimethylsilyl)oxy)phenyl]-4-chlorobenzenesulfonamide (**2**)

The initial 2-((trimethylsilyl)oxy)aniline **5** was obtained in high yield by refluxing of mixture of *o*-aminophenol with 0.5 mol equivalent of hexamethyldisilazane. To the stirred mixture of **5** (2.6 g, 14.3 mmol) and triethylamine (1.7 g, 16.8 mmol) in benzene (50 ml) the solution of 4-chlorobenzene-1-sulfonyl chloride (3.0 g, 14.2 mmol) in benzene (30 ml) was added dropwise. The reaction mixture was stirred for 6 h with moderate heating (40–50 °C). After cooling to room temperature a precipitate of $Et_3N{\cdot}HCl$ was filtered off and washed with 50 ml of benzene. The solvent was evaporated in vacuo. A residue was washed with hexane (10 ml) and dried in vacuo. The resulted product was melt and after cooling the crystals of pure **2** were formed. After the crystals were mechanically isolated from dark brown residue they were washed again with hexane (5–7 ml) and dried in vacuum. Almost pure product **2** was obtained in 82% yield (4.14 g).

2-((Trimethylsilyl)oxy)aniline **5**. ^{1}H NMR ($CDCl_3$, δ, ppm): 0.29 (s, 9H, $(CH_3)_3Si{-}O$), 3.68 (s, 2H, NH_2), 6.56–6.81 (m, 4H, Ar). Anal. calcd. for $C_9H_{15}NOSi$: C, 59.62; H, 8.34; N, 7.73. Found: C, 59.72; H, 8.49; N, 7.62.

N-[(2-trimethylsilyloxy)phenyl]-4-chlorobenzenesulfonamide (**2**): ^{1}H NMR ($CDCl_3$, δ, ppm): 0.17 (s, 9H, $(CH_3)_3Si{-}O$), 6.67–7.26 (m, 4H, 2-($OSiMe_3$)$C_6\underline{H}_4$), 7.47–7.80 (m, 4H, 4-$ClC_6\underline{H}_4$) ^{13}C NMR ($CDCl_3$, δ, ppm): 0.69 ($(\underline{C}H_3)_3Si{-}O$), 117.85 ($C_3$), 121.21 ($C_6$), 122.03 ($C_5$), 124.97 ($C_4$), 127.80 ($C_m$ 4-ClC_6H_4), 127.87 (C_1), 130.21 (C_o 4-ClC_6H_4), 137.41 (C_p 4-ClC_6H_4), 144.81 (C_i 4-ClC_6H_4), 145.45 (C_2). Anal. calcd. for $C_{15}H_{18}ClNO_3SSi$: C, 50.62; H, 5.10; N, 3.94. Found: C, 50.74; H, 5.43; N, 4.07.

The single crystals of **1** and **2** were obtained from melt.

2.2. X-ray study and refinement

Crystal data were collected on a Bruker D8 Venture diffractometer with MoK_α radiation ($\lambda = 0.71073$) using the φ and ω scans. Data collection: Bruker APEX2; cell refinement: Bruker SAINT; data reduction: Bruker SAINT. The structures were solved by direct methods using the SHELXS97 programs set (Sheldrick 2008) [43]. Data were corrected for absorption effects using the multi-scan method (SADABS). Non-hydrogen atoms were refined anisotropically using SHELXL2013 programs set (Sheldrick 2013) [43]. Software used to prepare material for publication e.g. molecular graphics: Bruker SHELXTL. Crystal data, data collection and structure refinement details are summarized in Table 1. **CCDC 1547521 (1)** and **CCDC 1547522 (2)** contain the supplementary crystallographic data for this paper. These data can be obtained free of charge from the Cambridge Crystallographic Data Centre via www.ccdc.cam.ac.uk/data_request/cif.

2.3. Quantum chemical calculations

All calculations were performed using the Gaussian 09 suite of programs [44]. DFT calculations of the monomers and dimers of amides **1**, **2** were performed using M062X/6-311 + G** level of theory. NBO and MO analyses were performed using B3LYP potential and 6-311 + G** basis set. The biological activity spectra of studied compounds were assessed by the PASS Online Program (http://www.way2drug.com/PASSOnline/).

2.4. NMR spectroscopy

NMR spectra were recorded for 20% solutions in $CDCl_3$ on a Bruker 400 MHz instrument with cyclohexane as an internal standard.

2.5. IR spectroscopy

The FTIR spectra were taken on a FTIR Spectrometer Varian 3100. For crystal compounds the spectra were recorded in KBr

Table 1
Crystal data, details of intensity measurements, and structure refinement for compounds **1** and **2.**

Compound	1	2
Empirical formula	$C_{16}H_{21}NO_3SSi$	$C_{15}H_{18}ClNO_3SSi$
Formula weight/g·mol^{-1}	335.49	355.90
Crystal system	triclinic	monoclinic
Space group	P-1	P 21/n
a, *b*, *c*/Å	8.7017(4), 9.1126(4), 33.4085(13)	10.5126(8), 16.0560(14), 11.2538(10)
α, *β*, *γ*/°	94.989(1), 90.119(2), 102.370(2)	90, 113.774(3), 90
Volume/Å^3	2577.2(2)	1738.3(3)
Z	6	4
Density (calculated)/g·cm^{-3}	1.297	1.360
Absorptions coefficient/mm^{-1}	0.269	0.419
Radiation (*λ*/Å)	MoKα (0.71073)	$Mo_{K\alpha}$ (0.71073)
Temperature/K	100(2)	100(2)
2*Θ* range/°	4.60–60.16	4.70–60.12
Crystal size/mm	0.140 × 0.250 × 0.500	0.310 × 0.330 × 0.500
Crystal habit	colorless plate	colorless prism
F(000)	1068	744
Index ranges	$-12 \le h \le 12$, $-12 \le k \le 12$, $-47 \le l \le 47$	$-12 \le h \le 14$, $-22 \le k \le 22$, $-15 \le l \le 15$
Reflections collected	79451	55180
Independent reflections	15043	5091
Max. and min. transmission	0.6562/0.7460	0.6429/0.7460
Number of ref. parameters	607	202
R_1/wR_2 [$I > 2\sigma(I)$]	0.0510/0.1068	0.0353/0.0803
R_1/wR_2 (all data)	0.0814/0.1182	0.0510/0.0863
Goodness-of-fit on F^2	1.022	1.045
Largest diff. peak and hole/e·Å^{-3}	1.177/−0.799	0.722/−0.691
Weight scheme, $P=(F_o^2+2F_c^2)/3$	$w = 1/[\sigma^2(F_o^2)+(0.0423\ P)^2+ 2.8783\ P]$	$w = 1/[\sigma^2(F_o^2)+(0.0337\ P)^2+ 1.2474\ P]$

pellets. The spectra of solutions of compounds **1**, **2** in inert media (CCl_4, $CHCl_3$, CH_2Cl_2) were registered with different concentration (0.02 mol l^{-1} – 0.1 mol l^{-1}).

3. Results and discussion

3.1. Structural analysis

The molecular structures of amides **1** and **2** are depicted in Fig. 1 and Fig. 2. Crystal data, data collection and structure refinement details are summarized in Table 1. Principal bond distances, bond angles and torsion angles are presented in Table 2.

According to X-ray data, the unit cell of compound **1** includes six molecules. In the crystal, compound **1** forms three conformers having different geometry (Fig. 3). The major differences concern the position of trimethylsilyloxy group and sulfonamide moiety with respect to the aromatic ring. Thus, the torsion angle Si1–O1–C2–C3 in **1a** is 134.0(2)°, and O1–C2–C3–N1 angle is equal to 4.2(2)°. In molecule **1b**, angle Si2–O4–C22–C21 is −173.5(2)° and angle O4–C22–C21–N3 is 10.3(3)°. In molecule **1c** angles Si3–O7–C33–C34 and O7–C33–C34–N2 are equal to −175.2 (1)° and −2.9(2) respectively. Two types of associates are formed by these conformers in the crystal: a cyclic dimer consisting of two **1a** molecules connected by two equal intermolecular H-bonds with the length of 2.281 Å and a cyclic dimer formed by **1b** and **1c** molecules connected by H-bonds with the lengths of 2.187 and 2.426 Å (Fig. 4).

In contrast, the asymmetric cell of compound **2** include only one molecule and only one type of associates is formed in crystal – a symmetric cyclic dimer with the intermolecular H-bond having the length of 2.294 Å (Fig. 5). Torsion angle Si1–O1–C2–C3 in the molecules of compound **2** is equal to −170.86(1)° and angle O1–C2–C3–N1 – 5.23(2)°. Geometric structure of amide **2** is similar to that in molecule **1c**. Geometrical characteristics of the hydrogen bonds of amides **1** and **2** are given in Table 3. The analysis of the literature data showed that in other similar structures, the values of O–C–C–N and Si–O–C–C angles vary in the range of 0.46 ÷ 2.52 and 108.95 ÷ 129.95 respectively [45–47].

3.2. The FTIR study of self-association of amides *1* and *2*

In spite of notable differences in the crystal structure of compounds **1** and **2**, their FTIR spectra are rather similar. No absorption bands corresponding to vibrations of free NH groups were observed in the FTIR spectra in the solid state (KBr) or in solution, which suggests that the molecules of **1** are completely associated. In an inert non-polar medium (CCl_4) there are few distinct bands related to self-associated forms of **1**, while in more polar solvents like $CHCl_3$ or CH_2Cl_2 only one band is observed (Table 4). The same behavior was observed for compound **2**, except that in all solutions a higher-frequency band of free NH group (3419-3475 cm^{-1}) appeared.

Low-frequency band 3265-3272 cm^{-1} observed in KBr and CCl_4 for both **1** and **2**, apparently, corresponds to the cyclic dimers of these amides. The larger shift is caused by the existence of two H-bonds. A low dipole moment can explain a higher stability of these self-associates in non-polar media. In polar solvents the more polar linear self-associates become more stable. The shift of the bands is due to association of the NH groups of linear associates of **1** and **2** and is very similar in the amides – 3336-3351 and 3332-3349 cm^{-1} respectively. Moreover, in CCl_4 solutions the adsorption bands were

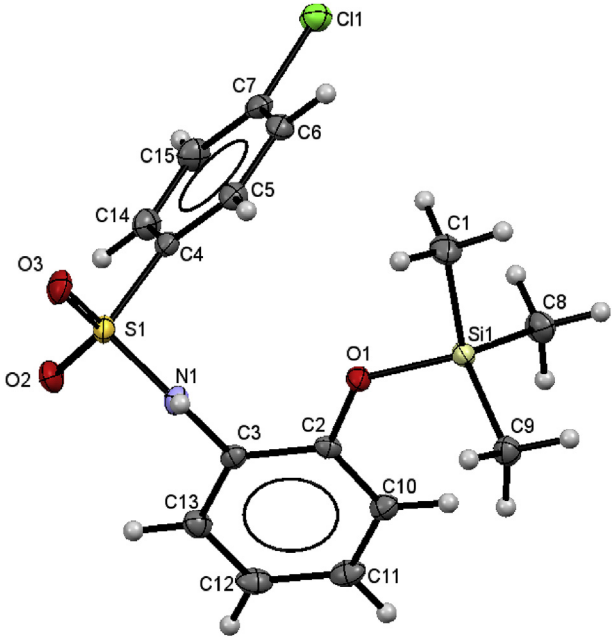

Fig. 2. Molecular structure of compound **2** (ORTEP, 50% probability ellipsoids).

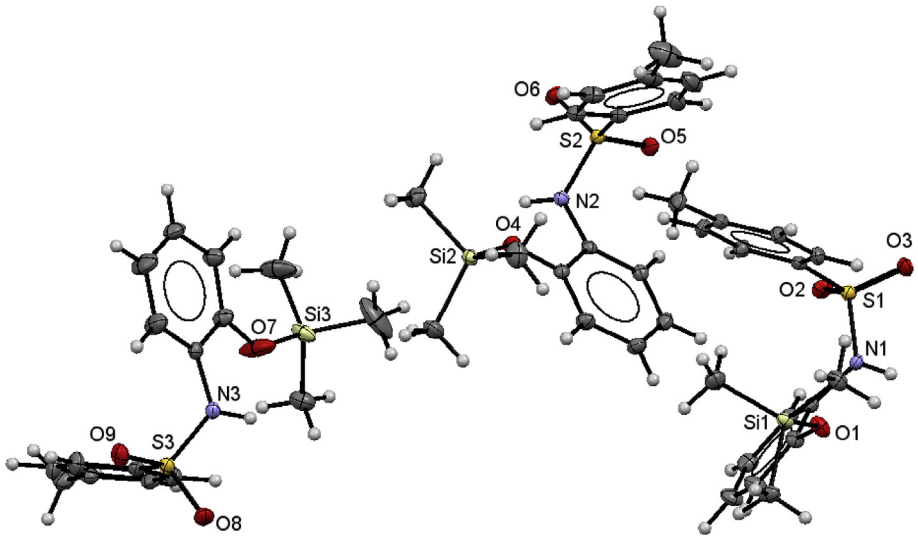

Fig. 1. Molecular structure of compound **1** (ORTEP, 50% probability ellipsoids).

Table 2
Selected bond lengths, bond and torsion angles in compound **1** and **2.**

Compound	Bond	*l*, Å	Angle	φ,°	Torsion angle	θ,°
1	S1–O2	1.438(1)	O3–S1–O3	119.6(1)	C8–Si1–O1–C2	−162.2(2)
	S1–N1	1.639(2)	O3–S1–N1	108.5(1)	C1–Si1–O1–C2	−40.8(2)
	S1–C35	1.760(2)	O3–S1–C35	108.7(1)	O3–S1–N1–C3	−46.4(2)
	S2–O5	1.434(2)	N1–S1–C35	106.9(1)	C35–S1–N1–C3	70.6(2)
	S2–N3	1.630(2)	O5–S2–N3	109.0(1)	O3–S1–C35–C14	−172.8(1)
	S2–C20	1.765(2)	O5–S2–C20	107.9(1)	N1–S1–C35–C14	70.3(1)
	S3–O9	1.440(1)	N3–S2–C20	107.5(1)	Si1–O1–C2–C3	134.0(2)
	S3–N2	1.635(2)	O9–S3–N2	105.1(1)	Si2–O4–C22–C31	7.8(4)
	S3–C36	1.766(2)	O9–S3–C36	109.4(1)	O5–S2–C20–C27	178.1(2)
	Si1–O1	1.677(2)	O1–Si1–C1	107.1(1)	N3–S2–C20–C19	−120.08(16)
	Si1–C1	1.866(2)	O4–Si2–C25	108.6(1)	Si3–O7–C33–C47	6.2(3)
	Si2–O4	1.659(2)	O7–Si3–C32	105.2(1)	N2–S3–C36–C43	129.4(2)
	Si2–C25	1.821(3)	C2–O1–Si1	125.8(1)	O9–S3–C36–C37	60.6(2)
	Si3–O7	1.674(1)	C3–N1–S1	122.9(1)	N2–S3–C36–C37	−52.2(2)
	Si3–C32	1.844(2)	C4–C35–S1	120.0(2)	N2–C34–C44–C45	−177.4(2)
	O1–C2	1.364(2)	C21–N3–S2	124.0(1)	C39–C42–C43–C36	0.8(3)
	N1–C3	1.430(2)	O9–S3–N2	105.1(1)	O7–C33–C47–C46	−179.8(2)
2	Cl1–C7	1.740(2)	O2–S1–O3	119.6(1)	C1–Si1–O1–C2	−178.6(1)
	S1–O2	1.433(1)	O2–S1–N1	108.9(1)	C8–Si1–O1–C2	−63.0(1)
	S1–O3	1.439(1)	O3–S1–N1	104.9(1)	C9–Si1–O1–C2	60.7(1)
	S1–N1	1.630(1)	O2–S1–C4	107.3(1)	O2–S1–N1–C3	−50.0(1)
	S1–C4	1.771(2)	O3–S1–C4	107.9(1)	O3–S1–N1–C3	−179.1(1)
	Si1–O1	1.683(1)	N1–S1–C4	107.8(1)	C4–S1–N1–C3	66.1(1)
	Si1–C1	1.851(2)	O1–Si1–C1	102.9(1)	Si1–O1–C2–C10	8.9(2)
	O1–C2	1.357(2)	C1–Si1–C9	113.3(1)	O1–C2–C3–C13	−178.6(1)
	N1–C3	1.430(2)	C2–O1–Si1	131.0(1)	C10–C2–C3–N1	−174.6(1)
	C2–C3	1.403(2)	C3–N1–S1	121.8(1)	S1–N1–C3–C13	64.6(2)
	C4–C5	1.391(2)	O1–C2–C3	116.9(1)	O2–S1–C4–C5	171.3(1)
	C5–C6	1.386(2)	C2–C3–N1	118.6(1)	C4–C5–C6–C7	−0.4(2)

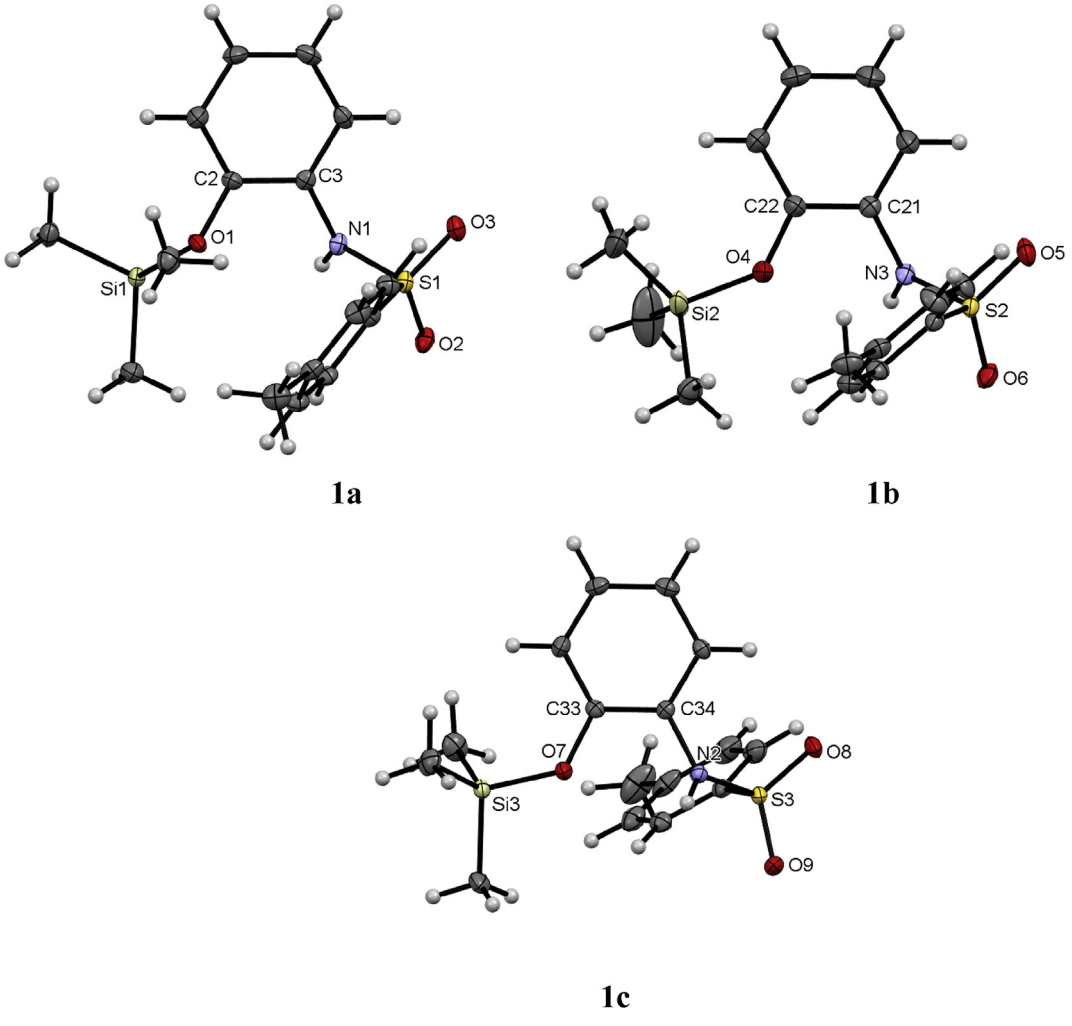

Fig. 3. Conformers of amide **1** in the crystal (**1a, 1b, 1c**).

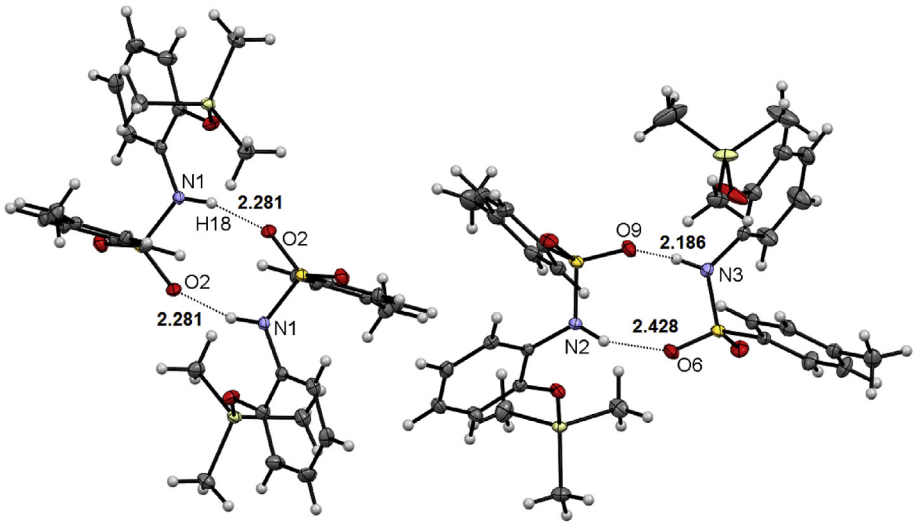

Fig. 4. H-bonded dimers of compound **1** in the crystal.

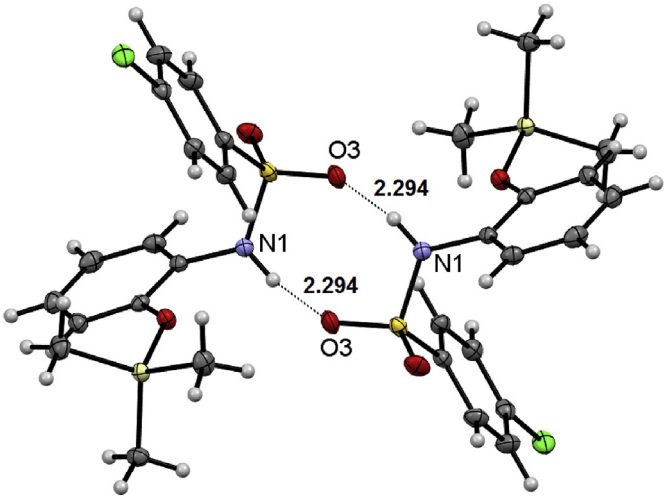

Fig. 5. H-bonded dimer of compound **2** in the crystal.

observed at 3385 cm^{-1} for compound **1** and 3379 cm^{-1} for compound **2**, which correspond to another linear associates that was formed. The H-bonds in the latter are weaker than in the aforementioned linear forms but it is stable in all examined solvents.

In order to determine the stability of conformers of compound **1** in the crystal, the intermolecular interactions in amides **1** and **2** in solution and the structure of their associates were investigated using quantum chemical calculations.

3.3. DFT calculations, QTAIM and NBO analyses, theoretical assessment of biological activity

Density functional theory (DFT) is the method for studying numerous systems, it has the balance of accuracy and efficiency. The B3LYP functional has been the method of choice for H-bonding interactions study in complicated biochemical systems such as peptides [48–50] and others [51–53]. The authors of the work [54] analyzed a lot new functionals introduced in the last few years among on those developed by Truhlar (M05, M05-2X, M06, M06-2X, and MPWB1K), Grimme (B2PLYP, B2PLYPD and B97D), and Goddard (X3LYP) in addition to B3LYP. M062X/6-311 + G** was called one from the best functional/basis set combinations that can be applicated for the complex H-bonded systems study [54].

In an attempt to evaluate the relative stability of the conformers of **1** existing in the asymmetric unit cell, the local minima on the potential energy surface were searched for. The initial geometries and atomic coordinates were taken from crystallographic data and then the geometry optimization was done at the M062X/6-311 + G** level of theory with frozen positions of heavy atoms and free protons. For comparison, the full geometry optimization was also performed at the same level of theory. The obtained data are summarized in Table 5.

According to calculations, conformer **1c** is the most energetically stable, while conformers **1a** and **1b** are less preferable by 5.0 and

Table 4
Experimental frequencies of free and associated NH-group (νNH, cm^{-1}) of compounds **1** and **2** in different media (KBr, CCl_4, $CHCl_3$, CH_2Cl_2).

Compound	KBr	CCl_4	$CHCl_3$	CH_2Cl_2
1	3336, 3268	3385, 3351, 3272	3352	3337
2	3475, 3265	3475, 3379, 3349, 3268	3419, 3342	3467, 3332

Table 5
Calculated energies of compound **1** conformers found in unit cell and fully optimized structure of **1** at M062X/6-311 + G** level of theory.

Structure	1a	1b	1c	1opt
- E, a.u.	1590.324983	1590.321986	1590.31709	1590.330756
ΔE (1opt-1x), kcal/mol	3.62	5.50	8.58	0

Table 3
Hydrogen bond distances (Å) and angles (°) for compounds **1** and **2**.

Compound	Bond	Donor-H	Acceptor-H	Donor-Acceptor	Angle	Symm.Codes
1	N1–H18···O2	0.880	2.281	2.962(2)	134.05	x,y,z; 2-x,-y,-z
	N2–H46···O6	0.880	2.428	3.064(2)	129.62	x,y,z; 1 + x,-1+y,z
	N3–H37···O9	0.879	2.188	2.899(2)	137.87	x,y,z; 1 + x,-1+y,z
2	N1–H14···O3	0.880	2.294	2.991(1)	136.12	x,y,z; 1-x,2-y,-z

Table 6
Bond lengths (*l*, Å), and calculated BCP properties (ρ(r), $\nabla^2\rho(r)$, *H*(r), V^e; au) and energies (E_{bond}, kcal/mol) for dimers of **1** and **2**.

Dimer	Bond	*L*	ρ(r)	$\nabla^2\rho(r)$	*H*(r)	V^e	E_{bond}
1a+1a	H···O	2.281	0.012345	0.051813	−0.002205	−0.008543	2.680379065
1b+1c	H···O(1)	2.187	0.014902	0.065195	−0.002778	−0.010743	3.370632365
	H···O(2)	2.426	0.009140	0.036614	−0.001499	−0.006156	1.931454234
2 + 2	H···O	2.294	0.011672	0.049048	−0.002138	−0.007985	2.505305728

3.1 kcal/mol, respectively (Table 5).

For each of two dimers, wave functions were generated (based on crystallographic coordinates at M062X/6-311 + G** level of theory) and QTAIM analysis was performed in order to evaluate the energies of H-bonds in the dimers. The self-associated form of compound **2** found in the crystal was also analyzed. Bond critical points (BCPs) in the molecules were found and their topological properties determined: the electron density ρ(r), the Laplacian of electron density $\nabla^2\rho(r)$, and the total energy densities *H*(r). The energies of interaction (*E*) were calculated by the equation $E_{bond} \approx -1/2V^e(r)$, where $V^e(r)$ is potential energy density in the corresponding BCP [55].

The calculated hydrogen bonding energy according to the AIM-analysis data correlates with the H-bond lengths in the dimers of amides **1** and **2** and with the values of the electron density and the Laplacian of electron density (Table 6). The values of formation energies of the dimers vary from 2 to 3 kcal/mol.

The molecular orbital (MO) analysis is broadly used to describe the electronic structure and chemical behavior of the different organic molecules including sulfonamides [34,56,57] and Si-containing compounds [36]. The MO analysis was used to study the electronic structure of compounds **1** and **2**. The calculated values of dipole moments, the energies of frontier molecular orbitals HOMO, LUMO and the HOMO–LUMO energy gaps Δ*E* of the studied molecules **1a**, **1b**, **1c** and **2** are summarized in Table 7. The frontier molecular orbitals for the studied molecules are graphically represented in Fig. 6. As can be seen from Fig. 6, in all molecules the HOMO is distributed on the phenyloxy fragment. The virtual orbitals LUMO are spread over the tosyl and chlorophenyl groups for amides **1** and **2**, respectively. The energy difference between frontier molecular orbitals (HOMO-LUMO), known as energy gap (*ΔE*), is a measure of the intramolecular charge transfer and is frequently used in chemical and biochemical activity studies. The high energy gap in chemical compounds would render their more stable towards ionization. The values of the HOMO–LUMO gaps (Δ*E*) show that the conformers of compound **1** are more stable than compound **2**, although both compounds have high enough values of Δ*E* (>5 eV), the chlorinated amide **2** being more reactive. Amides **1** and **2** have a *ΔE* value close to that in other benzosulfonamides studied earlier (5.22–5.55 eV) [56,57]. The dipole moments of conformers **1a**–**c** are higher than in compound **2**, suggesting higher hydrophobic properties of **1** as compared to **2**. The calculated second-order energies of electron delocalization $E^{(2)}$ related with the charge transfer from the lone electron pair of nitrogen on the antibonding C=O bond's π*-orbital are presented in Table 6. The energies of interactions $n_N \rightarrow \pi^*_{C=O}$ for compounds **1** and **2** fall in

Table 7
MO and NBO analysis data for compounds **1** and **2**.

Characteristics	Compound/conformer			
	1a	1b	1c	2
E_{LUMO}, eV	−1.30	−0.17	−1.14	−1.54
E_{HOMO}, eV	−6.48	−6.46	−6.38	−6.60
ΔE, eV	5.18	5.29	5.24	5.06
μ, D	7.24	7.44	7.19	6.32
$n_N \rightarrow \pi^*_{C=O}$, $E^{(2)}$, kcal/mol	7.08	9.46	8.54	8.03

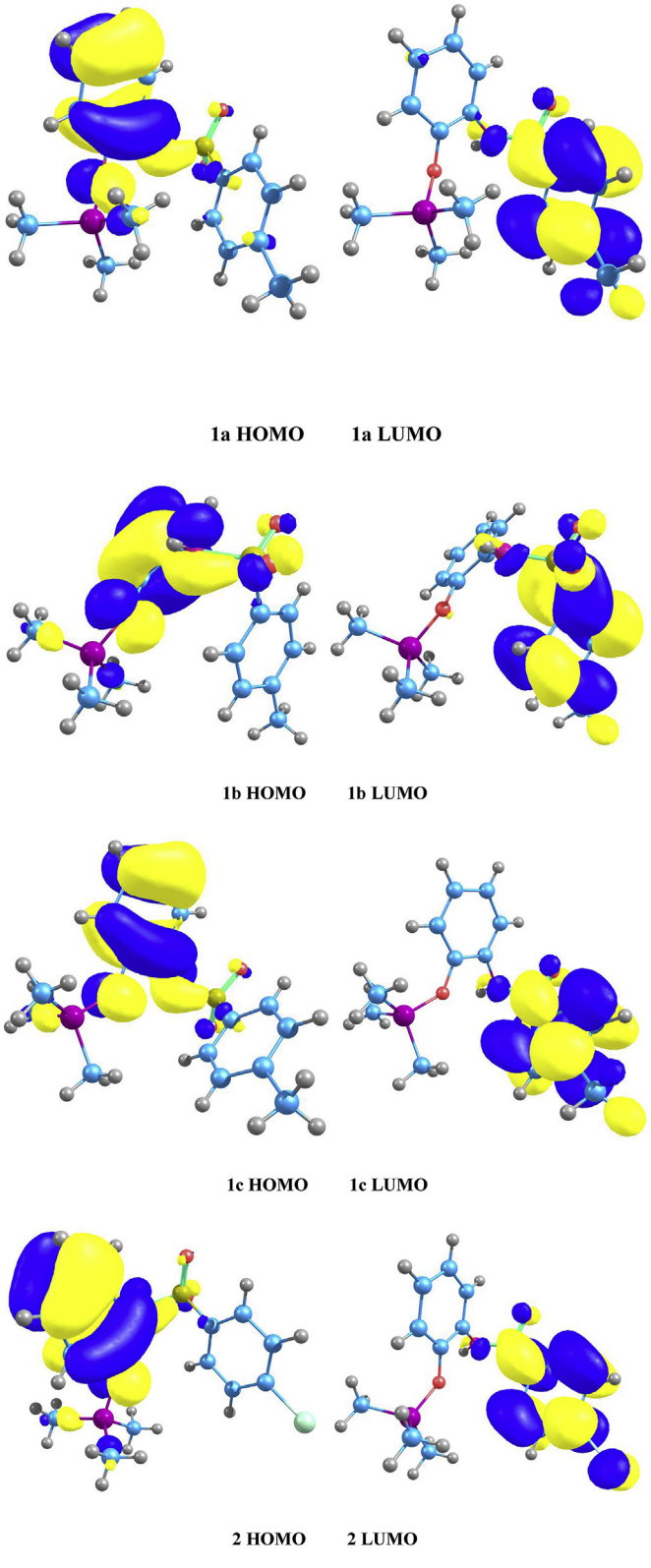

Fig. 6. Plots of frontier molecular orbitals for compounds **1** and **2**.

the range 7–9.5 kcal/mol, which is by 2–4 kcal/mol more than those found for the silylated sulfonamide and triflamide (5.5 kcal/mol), and by 1–3 kcal/mol less than in N-trimethylsilylbenzenesulfonamide (10.3 kcal/mol) [39].

The PASS Online Program was used to assess the biological activity of **1** and **2** and their isostructural carbon analogs [58]. According to the data of the PASS analysis, compounds **1** and **2** may show antiinfective (Pa = 0.69 and 0.65 for compounds **1** and **2** respectively) and antineoplastic (Pa = 0.56 and 0.50 for compounds **1** and **2** respectively) biological activity. In contrast of it isostructural carbon analogs show other types of biological activity (antidiabetic, antiobesity) and antiinfective activity to a lesser degree (Pa = 0.55 and 0.52) in comparison of amides **1** and **2**. That distinction is consistent with well-known fact that the introduction of the silicon atom in the molecule enhances lipophilicity of the molecule, which increases its bioaccessibility [59,60].

4. Conclusion

N-[(2-(Trimethylsilyl)oxy)phenyl]-4-methylbenzenesulfonamide **1** exists in the crystal in three forms having different geometry, whereas N-[(2-trimethylsilyloxy)phenyl]-4-chlorobenzenesulfonamide **2** shows only one molecular form. These differences are due to the packing effect on the structure of amide **1**. Theoretical calculations show that conformer **1c** is the most stable in comparison with conformers **1a** and **1b**. The QTAIM analysis gave only moderate energies of formation of the dimers of the studied compounds of 2–3 kcal/mol. The NBO analysis showed compound **2** to be more reactive and hydrophilic as compared to compound **1**.

Acknowledgements

Funding from the Russian Foundation for Basic Research (Grant No. 18-33-00368) is gratefully acknowledged. X-Ray data and FTIR spectra were obtained in the Collective Chemical Service Centre of SB RAS.

References

[1] S. Bhadra, H. Yamamoto, Chem. Rev. 118 (2018) 3391–3446.
[2] C. Sambiagio, D. Schönbauer, R. Blieck, T. Dao-Huy, G. Pototschnig, P. Schaaf, T. Wiesinger, M.F. Zia, J. Wencel-Delord, T. Besset, B.U.W. Maes, M. Schnürch, Chem. Soc. Rev. 47 (2018) 6603–6743.
[3] P. Ribiere, V. Declerck, J. Martinez, F. Lamaty, Chem. Rev. 106 (6) (2006) 2249–2269.
[4] J.D. Wilden, J. Chem. Res. 34 (10) (2010) 541–548.
[5] J.A. Halfen, Curr. Org. Chem. 9 (7) (2005) 657–669.
[6] H. Yang, R.G. Carter, Synlett 19 (2010) 2827–2838.
[7] F. Carta, C.T. Supuran, A. Scozzafava, Future Med. Chem. 6 (10) (2014) 1149–1165.
[8] T.V. Wani, S. Bua, P.S. Khude, A.H. Chowdhary, C.T. Supuran, M.P. Toraskar, J. Enzym. Inhib. Med. Chem. 33 (2018) 962–971.
[9] S.S.A. Shah, G. Rivera, M. Ashfaq, Mini Rev. Med. Chem. 13 (2013) 70–86.
[10] F.A. Scaffolds Khan, S. Mushtaq, S. Naz, U. Farooq, A. Zaidi, S. Bukhari, R.A. Majid, M.S. Mubarak, Curr. Org. Chem. 22 (8) (2018) 818–830.
[11] I. Melnikova, Nat. Rev. Drug Discov. 4 (2005) 453–454.
[12] A. Bertolini, A. Ottani, M. Sandrini, Curr. Med. Chem. 9 (2002) 1033–1043.
[13] J. Dong, Y. Wang, Q. Xiang, X. Lv, W. Weng, Q. Zeng, Adv. Synth. Catal. 355 (2013) 692–696.
[14] D.-W. Zhang, X. Zhao, J.-L. Hou, Z.-T. Li, Chem. Rev. 112 (2012) 5271–5316.
[15] N.N. Farshori, A. Ahmad, A.U. Khan, A. Rauf, Eur. J. Med. Chem. 46 (2011) 1433–1438.
[16] P. Panini, R.G. Gonnade, D. Chopra, New J. Chem. 40 (2016) 4981–5001.
[17] M. Abdoli, A. Angeli, M. Bozdag, F. Carta, A. Kakanejadifard, H. Saeidian, C.T. Supuran, J. Enzym. Inhib. Med. Chem. 32 (1) (2017) 1071–1078.
[18] M. Ashfaq, S. Shoaib A. Shah, T. Najjam, S. Shaheen, G. Rivera, Mini-Reviews Org. Chem. 10 (2013) 160.
[19] F. Carta, A. Scozzafava, C.T. Supuran, Expert Opin. Ther. Pat. 22 (2012) 747–758.
[20] C. Bissantz, B. Kuhn, M. Stahl, J. Med. Chem. 53 (14) (2010) 5061–5084.
[21] B. Kuhn, P. Mohr, M. Stahl, J. Med. Chem. 53 (6) (2010) 2601–2611.
[22] S.P. Maddaford, Methods Mol. Biol. 841 (2012) 351–381.
[23] J. Mortier, C. Rakers, M. Bermudez, M.S. Murgueitio, S. Riniker, G. Wolber, Drug Discov. Today 20 (6) (2015) 686–702.
[24] H. Zhao, A. Caflisch, Eur. J. Med. Chem. 91 (2015) 4–14.
[25] L.W. Tari (Ed.), Structure-Based Drug Discovery, Springer, New York, 2012, p. 385.
[26] S. Scheiner (Ed.), Noncovalent Forces, Springer, Cham Heidelberg, 2015, p. 528.
[27] N.A. Meanwell, J. Med. Chem. 54 (2011) 2529–2591.
[28] J.S. Mills, G.A. Showell, Expert Opin. Investig. Drugs 13 (2004) 1149–1157.
[29] A.K. Franz, S.O. Wilson, J. Med. Chem. 56 (2013) 388–405.
[30] I.V. Sterkhova, B.A. Shainyan, J. Phys. Org. Chem. 28 (2015) 485–489.
[31] I.V. Sterkhova, V.V. Astakhova, B.A. Shainyan, J. Mol. Struct. 1141 (2017) 351–356.
[32] N.F. Lazareva, A.Yu Nikonov, N.N. Chipanina, L.P. Oznobikhina, I.V. Sterkhova, A.I. Albanov, J. Organomet. Chem. 846 (2017) 88–99.
[33] A.Yu Nikonov, I.V. Sterkhova, I.M. Lazarev, A.I. Albanov, N.F. Lazareva, J. Mol. Struct. 1122 (2016) 10–17.
[34] H. Saeidian, H. Sadighian, M. Abdoli, M. Sahandi, J. Mol. Struct. 1131 (2017) 73–78.
[35] E. Taheri, Z. Mirjafary, H. Saeidian, J. Mol. Struct. 1157 (2018) 418–424.
[36] M.-F. Zaltariov, C. Cojocaru, S. Shova, L. Sacarescu, M. Cazacu, J. Mol. Struct. 1120 (2016) 302–316.
[37] N.N. Chipanina, N.F. Lazareva, T.N. Aksamentova, A. Yu Nikonov, B.A. Shainyan, Organometallics 33 (10) (2014) 2641–2652.
[38] I.V. Sterkhova, A.Yu Nikonov, I.M. Lazarev, V.I. Smirnov, N.F. Lazareva, J. Mol. Struct. 1098 (2015) 408–415.
[39] I.V. Sterkhova, A. Yu Nikonov, I.M. Lazarev, M. Yu Moskalik, N.F. Lazareva, Russ. J. Gen. Chem. 85 (2015) 1661–1667.
[40] W.L.F. Armarego, C.L.L. Chai, Purification of Laboratory Chemicals, sixth ed., Elsevier, 2009.
[41] K. Kurita, Chem. Ind. (London) (1974) 345.
[42] K.K. Andersen, G. Godwa, L. Jewell, P. McGraw, B.T. Phillips, J. Org. Chem. 47 (1982) 1884.
[43] G.M. Sheldrick, Acta Crystallogr. D64 (2008) 112–122.
[44] Gaussian 09, Revision A.01, M.J. Frisch, G.W. Trucks, H.B. Schlegel, G.E. Scuseria, M.A. Robb, J.R. Cheeseman, J.A. Montgomery Jr., T. Vreven, K.N. Kudin, J.C. Burant, J.M. Millam, S.S. Iyengar, J. Tomasi, V. Barone, B. Mennucci, M. Cossi, G. Scalmani, N. Rega, G.A. Petersson, H. Nakatsuji, M. Hada, M. Ehara, K. Toyota, R. Fukuda, J. Hasegawa, M. Ishida, T. Nakajima, Y. Honda, O. Kitao, H. Nakai, M. Klene, X. Li, J.E. Knox, H.P. Hratchian, J.B. Cross, V. Bakken, C. Adamo, J. Jaramillo, R. Gomperts, R.E. Stratmann, O. Yazyev, A.J. Austin, R. Cammi, C. Pomelli, J.W. Ochterski, P.Y. Ayala, K. Morokuma, G.A. Voth, P. Salvador, J.J. Dannenberg, V.G. Zakrzewski, S. Dapprich, A.D. Daniels, M.C. Strain, O. Farkas, D.K. Malick, A.D. Rabuck, K. Raghavachari, J.B. Foresman, J.V. Ortiz, Q. Cui, A.G. Baboul, S. Clifford, J. Cioslowski, B.B. Stefanov, G. Liu, A. Liashenko, P. Piskorz, I. Komaromi, R.L. Martin, D.J. Fox, T. Keith, M.A. Al-Laham, C.Y. Peng, A. Nanayakkara, M. Challacombe, P.M.W. Gill, B. Johnson, W. Chen, M.W. Wong, C. Gonzalez, J.A. Pople, Gaussian, Inc, 2009. Wallingford CT.
[45] J. Wagler, A.F. Hill, Organometallics 27 (2008) 6579–6586.
[46] H. Jaing, A.K. Kakkar, A.-M. Labuis, H. Zhou, G.K. Wong, J. Mater. Chem. 6 (1996) 1075.
[47] J. Wagler, A.F. Hill, CSD Communication, 2009. CCDC 725859.
[48] Y.-f. Chen, J.J. Dannenberg, J. Am. Chem. Soc. 128 (2006) 8100–8101.
[49] M.-H. Tsai, Y. Xu, J.J. Dannenberg, J. Phys. Chem. B. 113 (1) (2009) 309–318.
[50] D.-l. Wu, L. Liu, G.-f. Liu, D.-z. Jia, J. Phys. Chem. A 111 (24) (2007) 5244–5252.
[51] V.K. Palfi, A. Perczel, J. Comput. Chem. 29 (9) (2008) 1374–1386.
[52] D. Toroz, T.V. Mourik, Phys. Chem. Chem. Phys. 12 (14) (2010) 3463–3473.
[53] A. Bahrami, M.D. Esrafili, N.L. Hadipour, Biophys. Chem. 143 (1–2) (2009) 26–33.
[54] J.A. Plumley, J.J. Dannenberg, J. Comput. Chem. 32 (8) (2011) 1519–1527.
[55] E. Espinosa, E. Molins, C. Lecomte, Chem. Phys. Lett. 285 (1998) 170–173.
[56] A. Mahmood, T. Akram, E.B. de Lima, J. Mol. Struct. 1108 (2016) 496–507.
[57] A.G. Al-Sehemi, JK Sci. 23 (2011) 63–78.
[58] D.A. Filimonov, V.V. Poroikov, Probabilistic Approach in Activity Prediction, RSC Publishing, Cambridge, 2008, pp. 182–216.
[59] S. Gately, R. West, Drug Dev. Res. 68 (2007) 156–163.
[60] G.G. Changdev, J.C. Seung, J. Chosun Natural Science 5 (4) (2012) 229–232.